Published: 26 February 2025

Citation in BibTeX format

HOTMOBILE '25: The 26th International Workshop on Mobile Computing Systems and Applications
February 26 - 27, 2025
CA, La Quinta, USA

Conference Sponsors:
SIGMOBILE

RESEARCH-ARTICLE

RFBridge: Ultra Wideband Reconfigurable Metamaterial Surface Enabling Frequency Conversion

YAWEN LIU, Carnegie Mellon University, Pittsburgh, PA, United States

SHIVANG AGGARWAL, HP Labs, Palo Alto, CA, United States

MOHAMED IBRAHIM, HP Labs, Palo Alto, CA, United States

PUNEET SHARMA, HP Labs, Palo Alto, CA, United States

SWARUN KUMAR, Carnegie Mellon University, Pittsburgh, PA, United States

HotMobile '25: Proceedings of the 26th International Workshop on Mobile Computing Systems and Applications (February 2025)
https://doi.org/10.1145/3708468.3711884
ISBN: 9798400714030

RFBridge: Ultra Wideband Reconfigurable Metamaterial Surface Enabling Frequency Conversion

Yawen Liu[†], Shivang Aggarwal[‡], Mohamed Ibrahim[‡], Puneet Sharma[‡], Swarun Kumar[†*]
[†]Carnegie Mellon University, [‡]Hewlett Packard Labs

Abstract

This paper proposes a new capability for RF metasurfaces: highly programmable frequency conversion. We design RFBridge, a low-power metasurface that can simply convert RF signals on one frequency to another, with both of these frequency bands being highly configurable over a wide range – from 2 GHz to 8 GHz. We design this system as a means to open up varied applications for both wireless communication and sensing. Consider, for example, an RFBridge surface that acts as a frequency-converting relay from a 5 GHz Wi-Fi radio to a legacy 2.4 GHz Wi-Fi radio. Or consider multiple RFBridge surfaces that can collaboratively convert RF signals from a base station to various frequency bands in different rooms to minimize interference. We present a detailed design of RFBridge's frequency tunability and beamforming meta-cells, provide promising results through HFSS simulations, and discuss the exciting new applications opened up by frequency converting metamaterial surfaces.

CCS Concepts

• **Hardware → Wireless devices**; **Analysis and design of emerging devices and systems**.

Keywords

Metasurface, Metamaterials, Reconfigurable Intelligent Surfaces, Wireless Networks.

ACM Reference Format:
Yawen Liu[†], Shivang Aggarwal[‡], Mohamed Ibrahim[‡], Puneet Sharma[‡], Swarun Kumar[†]. 2025. RFBridge: Ultra Wideband Reconfigurable Metamaterial Surface Enabling Frequency Conversion. In *The 26th International Workshop on Mobile Computing Systems and Applications (HOTMOBILE '25), February 26–27, 2025, La Quinta, CA, USA.* ACM, New York, NY, USA, 6 pages. https://doi.org/10.1145/3708468.3711884

1 Introduction

In this paper, we ask – "Can we build a low-power metasurface that can simply convert RF waves from one frequency band to another, with both bands being entirely user-programmable?". Recent years have witnessed rich literature on smart surfaces for improving the coverage of wireless networks. They are often designed to be seamlessly attached to walls, while consuming minimal power unlike relays or additional access points. Their overall objective is to beam-steer signals in a manner that maximizes signal quality from transmitters to receivers, without posing significant complexity on either. Indeed, rich prior work exists on low-power metasurfaces of varied designs operating in wide-ranging frequency bands [4, 5, 10, 11]. In this work, we explore the potential of an entirely new capability of smart surfaces – configurable frequency conversion from one band to another.

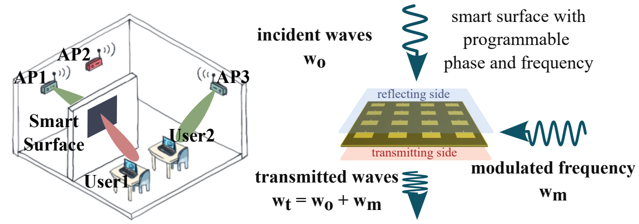

Figure 1: Motivation of RFBridge: frequency conversion for relay and beamform, to offload congestion or perform sensing for better spectrum management.

Indeed, programmable frequency conversion opens up a new range of applications for smart surfaces. Consider a surface that converts signals from an access point operating in one room (see Fig. 1) at one frequency band into another to reach a client in a neighboring room, where the original frequency band is congested. Or, consider a surface that interconnects a Wi-Fi access point operating at 5 GHz to a legacy device operating at 2.4 GHz. On the other hand, conventional relays and mixers are non-linear and thus they require high-power filters and amplifiers for signal fidelity across various bands. We envision building a highly integrated system that can adapt to diverse use cases, such as alleviating network congestion, providing cost-effective backhaul solutions, and performing dynamic spectrum management.

We present RFBridge, a reconfigurable low-power metasurface that enables frequency conversion between any two bands of interest within a wide range: from 2 GHz to 8 GHz. RFBridge allows both the incoming and outgoing frequency of operation to be fully programmable. In addition, RFBridge supports beam steering, i.e., spatially directing frequency-converted beams toward clients. We design and evaluate RFBridge through ANSYS High Frequency Structure Simulator (HFSS) simulations, demonstrating promising frequency tunability and conversion performance. Table 1 compares the capabilities of RFBridge with state-of-the-art metasurfaces. Prior work focuses on beam control but underexplores frequency manipulations. To the best of our knowledge, RFBridge is the first such metasurface that performs frequency conversion while simultaneously allowing ultra-wideband frequency programmability.

At the core of RFBridge are new solutions to program the metamaterial's resonant frequencies such that it naturally reflects or transmits the beam at the desired frequencies of interest. We achieve

[*]Yawen Liu did this work as an intern at Hewlett Packard Labs.

HOTMOBILE '25, February 26–27, 2025, La Quinta, CA, USA

ACM ISBN 979-8-4007-1403-0/25/02
https://doi.org/10.1145/3708468.3711884

Table 1: Comparison with state-of-the-art. *Limited efficiency and bandwidth; † Discrete, pre-defined frequencies

Specifications	RFLens [5]	TRI [10]	RFBouncer [11]	[12]	mmWall [4]	SIPS [16]	RFBridge
Operating bands	5 GHz	3.5 GHz	2.4 and 5 GHz	5-8 GHz	24GHz	1.8-5 GHz	2-8GHz
Dual-band operation	No	No	Yes	No	No	Yes	Yes
Frequency modulation	No	No	No	Yes	No	No	Yes
Frequency conversion	No	No	No	No	Partially*	Partially†	Yes
Beam control	Yes	Yes	Yes	Yes	Yes	No	Yes
Function versatility	transmitted	both	reflected	reflected	both	transmitted	both

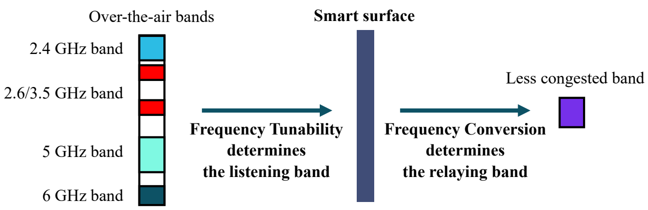

Figure 2: The two main functionalities: frequency modulation and frequency conversion; the arrow indicates signal direction.

this through a novel mechanism to achieve a mixer-like effect of the incident waves when interacting with the smart surface. Traditional frequency conversion systems, such as relays, rely on non-linear mixers that often produce spurious harmonics that degrade the signal quality. Instead, RFBridge's surfaces modulate the permittivity of the medium through digital control to achieve a near-linear mixing of the signals, enhancing frequency flexibility and seamless integration between frequencies. In doing so, RFBridge achieves robust frequency conversion over a wide bandwidth, while supporting some of the best-known properties of metasurfaces, such as beam steering.

2 Design Challenges and Solutions

In this section, we summarize the key design challenges in crafting RFBridge's metamaterial cells – the constituent elements of the metasurface.

Challenge 1: How does RFBridge achieve frequency conversion over an extremely large range of 2-8 GHz? Ensuring each metamaterial cell responds to a diverse, yet programmable range of frequencies is a key feature of RFBridge. However, enabling metasurfaces to programmatically tune over several gigahertz (specifically, 2-8 GHz) is challenging due to varied wavelengths across these frequencies. The naive approach of simply stacking multiple antenna structures is infeasible, given that each antenna size is proportional to the wavelength, which varies significantly across our desired range. Conventional wide-band antennas (around 5 GHz) such as U-slot, H-shape, or Vivaldi [2, 3] lack efficiency at the extremities of their bandwidth and offer limited phase control.

Solution 1: Frequency-tunable Cells. In contrast to these solutions, RFBridge opts for frequency-tunable rather than wide-band, allowing the surface to receive incident waves at programmable frequencies, as illustrated in Fig. 2. The surface can receive the incident signal and then relay it in the direction of the arrow. We achieve it by creating an unbalanced electric field within the metamaterial cell, where a pair of PIN diodes modulate the equivalent electrical length, thereby shifting the resonant frequency. §3.1 elaborates on our cell design and §3.2 demonstrates how it achieves frequency tunability.

Challenge 2: How can RFBridge achieve frequency conversion? Frequency conversion enables RFBridge to receive the incident waves and relay the signal at a programmable frequency. However, traditional frequency conversion requires conventional mixers that are power-hungry.

Solution 2: Space-Time Modulation. RFBridge achieves the effect of frequency mixing by designing unit cells that actively modulate the signal, not only in time, but also spatially, i.e., across cells. In other words, each unit cell induces signal amplitude and phase shifts that are carefully coordinated across cells by controlling bias-voltages with a time-varying magnitude at the PIN diodes, in a manner that emulates frequency shifts. We further design this system to suppress unnecessary harmonics. §3.3 elaborates on our approach. §3.4 extends this design to allow metasurfaces that enable frequency mixing either when the signal reflects off these surfaces (e.g., metasurfaces on walls bordering the exterior of a building) or when they propagate through (e.g., metasurfaces on walls separating rooms), as desired based on network topology.

3 Metasurface Design

RFBridge is a programmable metamaterial surface that operates at multiple frequency bands. In this section, we introduce the unit cell design to achieve frequency tunability, frequency conversion, and phase control in both transmitted and reflective modes.

3.1 Unit Cell Architecture

As shown in Fig. 3, the final unit cell design consists of four metal layers and three layers of FR4 substrates (relative permittivity ϵ_r = 4.4). The upper surface with a patch loaded by two slots on the sides is referred to as the **receiving antenna**, and the bottom surface with the O-slot patch antenna is referred to as the **transmitting antenna**. The transmitting antenna is connected to the ground plane at the second layer using via-holes. A ground plane is inserted to isolate the radiation between the top and bottom of the surface. We route the DC bias lines for diode control with a stub filter to ensure signal integrity and prevent RF-DC interference.

3.2 Enabling Frequency Tunability

In this section, we explain how to achieve frequency tunability of our unit cell. The diodes at the top *receiving antenna* determine the receiving frequencies in both reflective and transmissive modes,

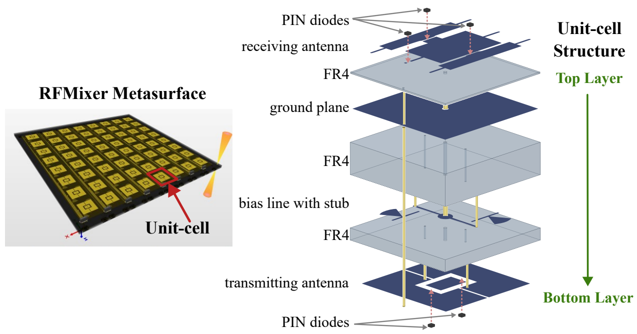

Figure 3: The RFBridge smart surface and structure of the proposed metamaterial unit cell.

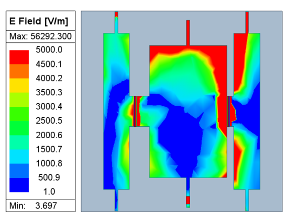

(a) Electric field intensity

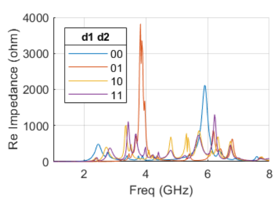

(b) Surface impedance

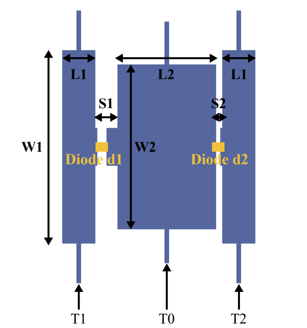

diode control (d1 d2)	Effective Width	Effective Length	Estimated Center Frequency
0 0	W2	L2	5.6 GHz
0 1	W1	L2+S2+L1	4 GHz
1 0	W1	L1+S1+L2	4.5 GHz
1 1	W1	2L1+L2+S1+S2	3.4 GHz

(c) Effective width and length

Figure 4: (a) Electric field intensity distribution changes when only diode d2 is switched on; (b) Surface impedance changes, when the diodes are turned on or off, indicating effective electrical length changes; (c) Physical width and length consideration of the unit cell; we define a diode to be "ON" (1) when a reverse bias is applied through the terminals and "OFF" (0) when no bias is applied.

inspired from [12]. When we apply reverse bias to both diodes, the center patch is effectively connected with the side microstrip to form an H-shape antenna structure. If only the right-side diode $d2$ (labeled in Fig. 4c) is switched on, the incident waves form an unbalanced electric field as in Fig. 4a, creating a non-uniform current flow. This results in perturbation of surface impedance across frequencies, as in Fig. 4b. The H-shape patch will start coupling with the other microstrip whose diode is off, lengthening the effective dimensions and lowering its resonance frequency.

Therefore, the key to ultra-wide frequency tunability is to consider the effective dimensions of the center and side patches when different diodes are turned on. We use a combination of mathematical analysis and HFSS simulation to develop a comprehensive design of the receiving antenna. The 2-bit control provides 4 configurations, collaboratively covering a wide bandwidth range, as shown in Fig. 4c. We estimate the resonant frequencies using the cavity model theory [9], such that $f = \frac{c}{2L_e\sqrt{\epsilon_{eff}}}$, where c is the free-space speed of light, ϵ_{eff} is the effective dielectric constant

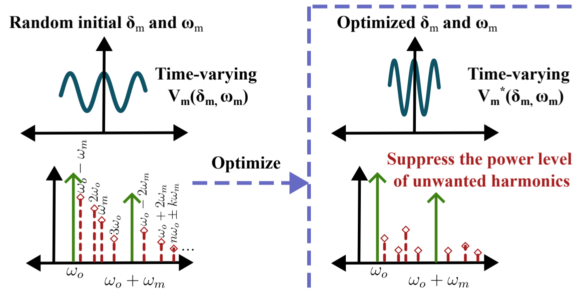

Figure 5: Schematic illustration of the frequency conversion and optimization problem.

(effective permittivity) of the substrate given as:

$$\epsilon_{eff} = \frac{\epsilon_r + 1}{2} + \frac{\epsilon_r - 1}{2}[1 + 12\frac{h}{w}]^{-1/2} \tag{1}$$

where ϵ_r is the relative dielectric constant of the substrate (ϵ_r = 4.4 for FR4), h is the height of the substrate and w is the physical width of the patch. The parameter L_e is the effective length of the patch such that:

$$L_e = l + 0.824h\frac{(\epsilon_{eff} + 0.3)(\frac{w}{h} + 0.264)}{(\epsilon_{eff} - 0.258)(\frac{w}{h} + 0.8)} \tag{2}$$

where l is the physical length of the patch.

In particular, we explore the sizing parameters using the above equations to initiate frequency control design. From Fig. 4c, the equivalent width and length w and l change as we turn the diodes on/off. We apply the reverse bias voltage to control the diodes through terminals T_1 and T_2, and terminal T_0 is their common anode. Using (1) and (2), we calculate the center frequencies for the 4 configurations to be 3.4, 4, 4.5, and 5.6 GHz which provide initial sizing parameters for our design. Our impedance simulation from HFSS in Fig. 4b matches the calculations in Fig. 4c, where a high impedance indicates a high reflection/transmission efficiency at that frequency. We further optimize the design in HFSS and evaluate frequency tunability in §4.

3.3 RFBridge Linear Frequency Conversion

To transform an incoming wave into a different relay frequency, RFBridge adopts an additional degree of freedom: *time*. Particularly, we leverage *space-time modulation* of the microstrip to achieve the desired mixing products of the waves [17]. This technique has been used widely for non-reciprocal RF devices [17, 18]. Space-time modulation alters both amplitude and phase of metamaterial cells simultaneously by controlling the bias voltage with a time-varying magnitude and frequency at a grounded PIN diode.

Inspired by the space-time modulated surface-interconnect-phaser-surface (SIPS) architecture [16], we use an additional diode on the receiving antenna to "mix" the incident waves. Let us define the time-varying control waveform as $V_m(\omega_m) = |V_m|cos(\omega_m t)$ with a modulation frequency ω_m. The permittivity couples when the incident wave with frequency ω_o propagates through the microstrip at position z and time t: $\epsilon(z,t) = \epsilon_r[1+\delta_m cos(\beta_m z - \omega_m t)]$, where δ_m is the amplitude of the modulated permittivity directly proportional to the amplitude of the control waveform $|V_m|$, and β_m and ω_m are the spatial frequency and temporal frequency. In other words, we continuously program $\epsilon(z,t)$ using V_m to introduce a

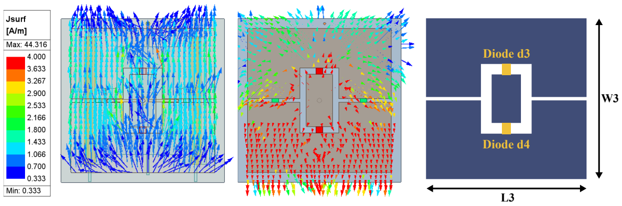

(a) The current distribution (b) Dimensions

Figure 6: (a) The current distribution changes when only one diode is turned on, indicating phase changes (left: d3 is ON; right: d4 is ON); (b) Physical width and length consideration of the transmitting antenna.

superposition of its frequency, with infinite modes of harmonics as the wave travels through and scatters between the metal layers.

Note that the above modulation yields harmonic products similar to conventional mixers, with undesired mixing products $n\beta_o \pm k\beta_m$ and $n\omega_o \pm k\omega_m$, for integer values of k and n. To suppress the undesired harmonics, RFBridge considers the dominant factors for precise signal mixing. First, we leverage the fact that sub-wavelength metamaterial structures introduce minimum phase constant variations owing to their small dimensions (i.e., position z). Consequently, the spatial frequencies $n\beta_o \pm k\beta_m$ become negligible due to the aforementioned phase values being small and constant. We therefore suppress the undesired mixing components and preserve the dominant frequency $n\omega_o \pm k\omega_m$.

To optimize this frequency conversion, we investigate the dominant factors from $\epsilon(z,t)$ to control the frequency relayed by the metasurface. The two main parameters are the amplitude δ_m (i.e., selecting the appropriate modulation amplitude $|V_m|$) and frequency ω_m. A small δ_m indicates energy concentrates in the fundamental component ω_o, and a large δ_m means much of the energy resides in the harmonic frequencies. While Bloch-Floquest's decomposition can provide a closed-loop solution of the electric field strength [17], we simplify this process into an optimization problem (Fig. 5). Our goal is to find the solution that defines the optimal waveform V_m^* to the following optimization problem:

$$V_m^*(\delta_m, \omega_m) = \underset{\delta_m, \omega_m}{\operatorname{argmax}} |V_t(\omega_t)|^2 \tag{3}$$

where V_m^* is an optimal solution that programs the incident wave to the desired frequency $\omega_t = \omega_o + \omega_m$ with maximum signal power for the relay signal V_t. RFBridge runs voltage waveform sweeping for this optimization. We supply this modulation waveform using a digitally programmable voltage-controlled oscillator (VCO) and use a multi-way power divider to load cells with equal voltages.

3.4 RFBridge Mode Switching

RFBridge achieves mode switching and phase control using the interconnected structure to alter the current flow direction. The transmitting antenna has an O-slot ring and two diodes connected to the center island port as in Fig. 6b. This symmetric pair of diodes determines the phase and operating mode of RFBridge, by blocking/allowing the current flow captured by the receiving antenna into the ring. If we switch on exactly one diode, either d3 or d4, the two current distributions of the O-slot resonator have opposite directions as illustrated in Fig. 6a, indicating a phase difference of 180° in the waves radiating out. If neither of the two diodes is on, minimum current will leak into the ring, thus radiating minimum power. We size the transmitting antenna using (1) and (2) at 2.5 GHz to provide higher transmitted efficiency covering the frequency gaps from Fig. 4c. We evaluate the scattering parameters (S-parameters) between different configurations and demonstrate the frequency tunability, mode switching, and phase control in §4.

4 Preliminary Results

To evaluate RFBridge's ability to beam and relay signals at configurable frequencies, we run HFSS simulations with 10×10 unit cells (surface area of 250×250 mm^2). While HFSS cannot handle voltage modulation in transient simulation over a wide bandwidth, we consider the frequency conversion efficiency via the radiation pattern at the converted frequency assumed near-linear conversions.

Frequency tunability. We evaluate the S-parameter in Fig. 7 and phase offset across our targeted bands. Fig. 7b and Fig. 7d show the configurations for the reflection mode, and Fig. 7c and Fig. 7e for the transmission mode. We compare the S-parameter with the frequency modulation diode switched on/off, with a negligible influence on the center frequency during frequency conversion. We summarize the tunable frequency ranges with a cutoff of -6 dB in the S11 and S21 magnitude (50% energy is reflected/transmitted) in Table 7a and corresponding diode configurations and modes.

The reflection frequency is programmable from 2-8 GHz with independent phase controls; the transmission frequency is programmable from 2.4-8 GHz with a frequency conversion modulation wave range up to 4.4 GHz from the VCO, i.e., an incidence ω_o = 2.4 GHz can be converted up to harmonics at $\omega_t = \omega_o + \omega_m$ = 6.8 GHz within the transmission frequency range. We note that there are limitations where the reflection and transmission amplitude are weaker than -6 dB or phase shifts less than $1/2\pi$, which may degrade performance at these frequency gaps (e.g., 6.2-6.8 GHz for reflection and 4.2-5 GHz for transmission). We find that RFBridge can effectively manipulate 86.7% and 90% of the targeted bands overlapping from 2 to 8 GHz for reflection and transmission.

Independent phase control. Note that our 4-bit diodes control both operating frequency and phase shifts. Hence, instead of calculating phase quantization as in prior work [5, 11], RFBridge finds the *overlapping frequency and phase shifts between two configurations*. We need to carefully select the operating frequencies based on Table 7a, having all 4-bit diodes collaboratively create a discrete phase shift between the adjacent cells' absolute phase values. We use a phase quantization to simplify the beam steering - a phase offset in the range $0 < \phi < \pi$ is considered as π and in the range $\pi < \phi < 2\pi$ is considered as 2π. For instance, in reflection mode, when one cell is set to d1d2 = 00 and its neighboring cell is set to d1d2 = 10, both operate at 5.5 GHz and their phase offset is $\simeq 2\pi$ (Fig. 7d). Similarly, a combination of d1d2 = 10 and d1d2 = 11 in transmission mode with d3d4 = 01 has a phase offset $\simeq \pi$ at 3.6 GHz (Fig. 7e). This frequency selection and phase quantization can degrade beamforming performance with increased complexity and lower steering accuracy, but such phase quantization has been proven by prior work to provide sufficient steering angle accuracy. We show the steering resolution for 10×10 unit cells RFBridge is

Diode States d1 d2	d3 d4	operating mode	frequency range with significant phase offset (GHz)
00	00	Reflection	2-6.3, 6.9-7.2
01	00	Reflection	2.4-2.6, 3.2-4, 4.2-4.4, 4.5-5.8, 6.9-7.2
10	00	Reflection	2.4-3.2, 4-4.6, 4.9-5.8, 6-6.6, 6.9-7.2
11	00	Reflection	2.6-7.2
00	01	Transmission	2.6-3.2, 4.3-4.5, 5-6.5, 7.2-8
01	01	Transmission	2.5-4.5, 5-6.5, 7-7.4, 7.7-8
10	01	Transmission	2.4-4.3, 4.4-6.2, 7-7.4, 7.7-8
11	01	Transmission	2.5-4, 7.4-8
00	10	Transmission	2.7-3, 5.3-6.5, 7-7.3
01	10	Transmission	2.5-4.6, 5-6.4, 7-7.3, 7.7-8
10	10	Transmission	2.4-4.2, 5-6.2, 7-7.3, 7.7-8
11	10	Transmission	2.4-4.2, 7-8

(a) Look-up table of surface modes and diode states

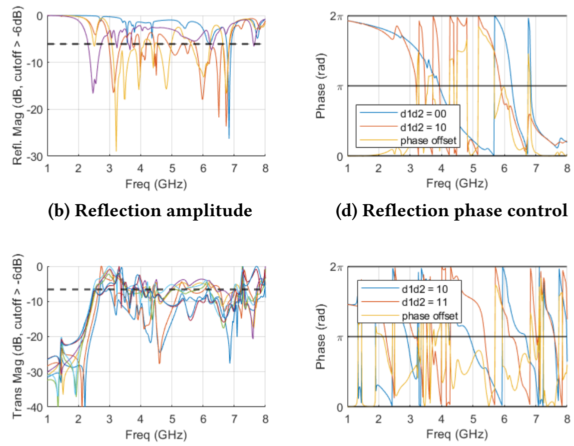

(b) Reflection amplitude **(d) Reflection phase control** **(c) Transmission amplitude** **(e) Transmission phase control**

Figure 7: The reflection and transmission amplitude of the unit-cell for two modes, alongside the correspondence between operating modes and 4-bit diode states, with examples of phase offsets control in (d) and (e).

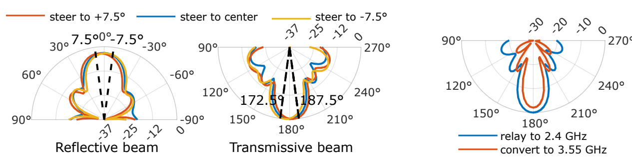

(a) Same-frequency beam resolution **(b) Converted beam**

Figure 8: (a) reflective and transmissive beam patterns at 2.4 GHz; (b) frequency converted beam at $\omega_o + \omega_m$.

$7.5°$ in Fig. 8. RFBridge thus can beam-steer across a wide range of frequencies, across the possible combinations.

Frequency conversion beam efficiency. Fig. 8 evaluates the beam steering performance of the two operating modes. We conduct HFSS simulation with an incident wave from the top of the surface at $0°$ to analyze the radiation patterns in Fig. 8a with the smallest beam steering resolution RFBridge can achieve ($7.5°$). RFBridge can achieve 90.4% and 95.4% efficiency for the same frequency reflection and transmission, indicating 0.44 dB and 0.21 dB loss when relaying or passing the signals. If we relay the signal at 2.4 GHz + 1.15 GHz (3.55 GHz), the peak power is 2.06 dB weaker compared to relaying at the same frequency 2.4 GHz, as shown in Fig. 8b.

5 Related Work

Metamaterial surfaces. Metamaterial surfaces have been explored to provide additional wireless signal programmability to resolve coverage problems. State-of-the-art designs focus on smart beamforming to improve channel quality for single/dual bands [11] and multiplexing [18]. RFLens helps beamform to small IoT devices with high beam steering accuracy [5] while RFBouncer enables beam control in two frequency bands [11]. However, their goal is intrinsically different from our objective of bridging networks operating on different frequency bands.

Heterogeneous Wireless Networks (HWN). The new wireless spectrum enables various types of wireless networks (5G, WiFi, etc.), enabling high data rates (multi-Gbps). HWN refers to the network architecture that integrates wireless networks for better connectivity and performance in scale. The main challenges for

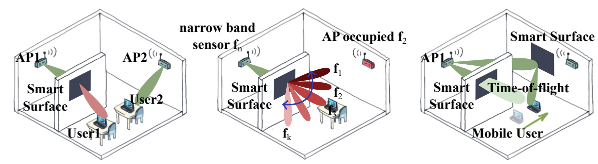

(a) Coverage extension **(b) Spectrum sensing** **(c) Path diversity for mobility**

Figure 9: Illustration of RFBridge use cases.

HWN come from the mobility of users, spatial distribution, and handovers. Mobile relays for 4G LTE and 5G New Radio leverage dual connectivity and relay nodes for reliable connections with mobility [13]. Massive MIMO [6] and relay systems [15] can effectively improve coverage in areas of poor signal at the cell edges. Coordinated multipoint (CoMP) involves multiple access points and base stations working together [13]; however, it requires a known overlap between cells and costly backhaul for coordination. RFBridge aims to address these problems by providing accessories that can bridge networks and improve spectrum efficiency when multiple access points (APs) and base stations are involved.

6 Extended Application

We believe RFBridge has significant potential to improve and extend wireless sensing and communication systems. Fig. 9 illustrates some potential applications we aim to develop based on RFBridge.

Coverage Extension. We have witnessed the advances of reconfigurable intelligent surface (RIS) in the past decade [5, 10–12]. However, these systems only support limited frequency bands. On the other hand, RFBridge can extend the coverage of a network operating in one frequency band to another, either to support legacy devices or to prevent interference in a region where the transmitter's band is crowded (Fig. 9a). RFBridge opens up new directions integrating multiple wireless networks with cross-band interoperability and frequency reuse.

Spectrum Sensing. Conventional spectrum sensing typically requires a wideband receiver or densely deployed narrowband receivers. Instead, RFBridge can collaboratively feed different wide RF bands $f_1, f_2, \ldots, f_k$ into a common narrow-band f_n. This enables a new approach to spectrum sensing with a narrowband receiver that can readily sense f_n to learn if any of the original bands $f_1, f_2, \ldots, f_k$ (Fig. 9b). In particular, RFBridge converts a unique, yet sparsely utilized, frequency band into a common narrowband in a short scanning interval – allowing spectrum sensing of wide bandwidths from a narrow band receiver. Thus, RFBridge can significantly reduce the costs of sensing receivers, offering more flexible spectrum utilization with a small trade-off of occupying a narrow channel at f_n for sensing purposes (e.g., CBRS, used for Private 5G, has 10 MHz channels and Wi-Fi 6 has 160 MHz channels).

Localization and Tracking. RFBridge can also benefit indoor RF localization where frequency shifting a user's signal leads to a wider effective bandwidth – a property that directly helps localization and tracking (specifically, time-of-flight based localization) systems (Fig. 9c). Applications such as automation of networked robots and mobile tracking, which involve enormous devices, also demand fast handover. RFBridge can address this challenge by reducing the cost of APs and improving handover at the coverage edges.

7 Discussion on Future Research

System Design. The high-level system architecture is similar to other metasurface systems: we assume the APs and sensing devices have prior knowledge of the metasurface location, embedded on furniture, ceiling, and/or walls. RFBridge can generate directional beams and simultaneously scan for optimal links to the device. Then, RFBridge can convert the signal to another frequency, relying entirely on pre-set modes, backed up by careful calibration. In multisurface or multiuser scenarios, lower sub-GHz frequencies can be used to exchange control signals between the APs and surfaces.

Dynamic access networks. The dynamic nature of frequency convertibility enables better management of spectrum and devices with diverse network types, such as Wi-Fi, IoT, and public/private cellular networks. We have previously discussed having RFBridge relay cross-band signals to integrate heterogeneous networks as dynamic access networks (DAN). Currently, there are various protocols for network co-existence. However, the idea of enabling information exchange among these networks is currently underexplored. Given the fast-growing complexity and scale of wireless networks, we envision a system that can increase the utilization of spectrum and the seamless integration of networks. To achieve this, the new DAN management requires shared standards and protocols to avoid compatibility issues – standards such as IEEE 1900.4s [1] have been proposed. A careful design of modulation and CSI is required to achieve direct message conversion through RFBridge, between two devices of different protocols, to minimize congestion. The potential opportunities here are to improve the scalability, utilization, and security of network integration.

Implementation. Although a single device can provide good coverage for spaces in homes/apartments, the implementation cost scales up fast with a large number of APs for enterprises or public spaces. Instead of deploying more state-of-the-art Wi-Fi 6/7 APs ($200 each) or 4G/5G CBRS base stations ($2,500 each) [14], RFBridge requires a printed circuit board using the FR4 substrate ($50) and diodes ($0.123 each and approximately $60 in total) [8]. We customize a control board with a microcontroller ($10) and a digitally programmable VCO ($30) to generate the modulation frequency [7]. Therefore, the total implementation cost ($140) of our prototype is still less than the deployment cost of mesh APs.

Power Consumption. Metasurface consumes significantly less power than conventional relay systems and beamforming arrays that leverage active RF electronics. RIS can be controlled with low-power diodes [8]. RFBridge requires one additional VCO compared to other metasurfaces [7]; on the contrary, a relay requires at least two local oscillators to downconvert and upconvert RF signals.

8 Conclusion

In this paper, we presented RFBridge, a novel metasurface that is capable of both frequency conversion as well as beamforming. We present the design and simulation results that showcase RFBridge's promise in operating over a wide frequency range (2-8 GHz) while being highly programmable. We demonstrated its promising capabilities through HFSS simulations. We will fabricate a RIS prototype of this design, and refine it for practical system implementation.

Acknowledgments: We thank NSF (2114733, 2030154, 2106921, 2007786) and the ONR for supporting this project.

References

[1] 2011. IEEE Standard for Architectural Building Blocks Enabling Network-Device Distributed Decision Making for Optimized Radio Resource Usage in Heterogeneous Wireless Access Networks Amendment 1: Architecture and Interfaces for Dynamic Spectrum Access Networks in White Space Frequency Bands. *IEEE Std 1900.4a-2011 (Amendment to IEEE Std 1900.4-2009)* (2011), 1–99.
[2] J. Borchardt and T. Lapointe. 2019. U-Slot Patch Antenna Principle and Design Methodology Using Characteristic Mode Analysis and Coupled Mode Theory. *IEEE Access* 7 (2019), 109375–109385.
[3] Y. Chen, Y. He, W. Li, L. Zhang, S. Wong, and A. Boag. 2021. A 3–9 GHz UWB High-Gain Conformal End-Fire Vivaldi Antenna Array. In *IEEE AP-S/URSI.* 737–738.
[4] K. Cho, M. Mazaheri, J. Gummeson, O. Abari, and K. Jamieson. 2023. mmWall: A Steerable, Transflective Metamaterial Surface for NextG mmWave Networks. In *Proc. of USENIX NSDI.*
[5] C. Feng, X. Li, Y. Zhang, X. Wang, L. Chang, F. Wang, X. Zhang, and X. Chen. 2021. RFlens: metasurface-enabled beamforming for IoT communication and sensing. In *ACM MobiCom.* 587–600.
[6] J. Gong, A. Kalia, and M. Yu. 2023. Scalable Distributed Massive MIMO Baseband Processing. In *Proc. of USENIX NSDI.*
[7] Analog Devices Inc. 2024. ADF4355-2BCPZ PLL 4.4GHz PLL w/integrated low noise VCO, Analog Devices. https://www.mouser.com/ProductDetail/Analog-Devices/ADF4355-2BCPZ?qs=hpwIUhX6lWz6eoM%2F3mmSQQ%3D%3D
[8] Skyworks Solutions Inc. 2024. SMP1340-040LF: Fast Switching-Speed, Low-Capacitance, Plastic-Packaged PIN Diodes. https://www.mouser.com/ProductDetail/Skyworks-Solutions-Inc/SMP1340-040LF?qs=WMHGlxXAKT+z1s6KsEgmuw%3D%3D
[9] J.R. James, P.S. Hall, and C. Wood. 1986. *Microstrip Antenna: Theory and Design.*
[10] G. Li, H. Shi, J. Yi, B. Li, A. Zhang, and Z. Xu. 2022. Transmission–Reflection-Integrated Metasurfaces Design for Simultaneous Manipulation of Phase and Amplitude. *IEEE Transactions on Antennas and Propagation* (2022).
[11] X. Li, C. Feng, X. Wang, Zhang Y., Y. Xie, and X. Chen. 2023. RF-Bouncer: A Programmable Dual-band Metasurface for Sub-6 Wireless Networks. In *Proc. of USENIX NSDI.*
[12] R. Phon, M. Lee, C. Lor, and S. Lim. 2023. Multifunctional reflective metasurface to independently and simultaneously control amplitude and phase with frequency tunability. *Advanced Optical Materials* 11, 14 (2023), 2202943.
[13] M. Sawahashi, Y. Kishiyama, A. Morimoto, D. Nishikawa, and M. Tanno. 2010. Coordinated multipoint transmission/reception techniques for LTE-advanced [Coordinated and Distributed MIMO]. *IEEE Wireless Communications* 17, 3 (2010), 26–34.
[14] Sercomm. 2025. Sercomm 5G Small Cell. https://www.sercomm.com/en/solutions/product/4/2/38
[15] V. Sreng, H. Yanikomeroglu, and D. Falconer. 2002. Coverage enhancement through two-hop relaying in cellular radio systems. In *Proc. of IEEE WCNC.*
[16] S. Taravati and G. Eleftheriades. 2021. Pure and linear frequency-conversion temporal metasurface. *Physical Review Applied* 15, 6 (2021), 064011.
[17] S. Taravati and A. Kishk. 2020. Space-Time Modulation: Principles and Applications. *IEEE Microwave Magazine* 21, 4 (2020), 30–56.
[18] X. Wang and C. Caloz. 2019. Spacetime-Modulated Metasurface for Spatial Multiplexing Communication. In *Metamaterials'2019.*